



# Analytical Solution to the Vinti Problem in Oblate Spheroidal Equinoctial Orbital Elements

Ashley D. Biria<sup>1</sup>  · Ryan P. Russell<sup>1</sup>

Published online: 21 May 2019  
© American Astronautical Society 2019

## Abstract

Equinoctial orbital elements were recently generalized from spherical geometry to the oblate spheroidal geometry of Vinti theory. For the symmetric Vinti potential, which accounts exactly for oblateness, these nonsingular elements are defined for all nondegenerate orbital regimes and resolve the usual problems found in the classical elements associated with angle ambiguities. In the present work, the generalized equinoctial elements are used to solve Vinti's initial value problem, leading to a fully nonsingular analytical solution for bounded orbits. The result is akin to deriving the equinoctial form of Kepler's equation for the two-body problem and then solving it, formally completing the introduction of the new equinoctial element set. Derivations of the equinoctial integrals of the motion are included, as well as techniques to eliminate all polar orbit singularities and solve a generalized Kepler's equation. Multiple examples are presented. Code for predicting the Vinti orbit in oblate spheroidal equinoctial elements is provided online as [supplementary material](#).

**Keywords** Equinoctial elements · Oblate bodies · Vinti theory · Spheroidal method · Analytical solution · Orbit prediction · Intermediary

## Introduction

A cursory glance at the astrodynamics landscape renders numerical methods indispensable and analytical methods obsolete. In reality, astrodynamics tools must keep

---

**Electronic supplementary material** The online version of this article (<https://doi.org/10.1007/s40295-019-00179-y>) contains supplementary material, which is available to authorized users.

---

✉ Ashley D. Biria  
[biria@utexas.edu](mailto:biria@utexas.edu)

Ryan P. Russell  
[ryan.russell@utexas.edu](mailto:ryan.russell@utexas.edu)

<sup>1</sup> Department of Aerospace Engineering and Engineering Mechanics, The University of Texas at Austin, 210 E. 24th St., Austin, TX 78712, USA

pace with increasingly complex missions. When the complexity stresses or breaks existing tools, a synergetic solution that leverages both approaches can be a viable option. One area that continues to use analytical methods is mission design, where analytical solutions can enable rapid searches of large design spaces and furnish good initial guesses to optimization software. Depending on the application, it can be beneficial to perform the orbit propagation with an analytical solution like the one presented in this paper. As the present solution includes oblateness, it would only be useful if oblateness is not negligible, such as for many-revolution scenarios. As an example, the authors used a modified Vinti propagator [14] in the ninth Global Trajectory Optimization Competition (GTOC 9)<sup>1</sup> to explore its applicability. In this case, oblateness was essential to the dynamics of the mission design problem, which required the active removal of 123 pieces of sun-synchronous debris from low Earth orbit. To save fuel, it may be beneficial for the spacecraft to spend 10 days in transit to the next piece of debris, exploiting oblateness effects to reach its target. Compared to an eighth order Runge-Kutta numerical integrator taking 50 steps per revolution, the analytical solution was found to offer a 400 times speed-up for that time of flight. The solution developed in this work would lead to qualitatively similar behavior. These types of speed-ups, manifested for certain applications and accuracy requirements, are among the advantages that motivate the further development of Vinti theory.

The Vinti [23, 28] gravitational potential, which constructs orbits on an oblate spheroidal geometry, is one of many so-called intermediaries, comprising a branch of literature in celestial mechanics. In general, intermediaries can lead to exact solutions to approximate problems. Perturbation methods [22], on the other hand, typically lead to approximate solutions to an exact problem. Contributions in the realm of spherical geometry include Cid and Lahulla's radial intermediary [12, 16, 21] and the development of a systematic approach to generating intermediaries to first order [15]. Biria [1] discusses various intermediaries in greater detail. In the realm of spheroidal geometry, a number of notable investigations into Vinti theory have been made in the last few years [32, 33, 35]; these works utilized the symmetric Vinti potential (oblateness without  $J_3$ ) and addressed methods of solution, incorporation of drag, the study of resonances in the rotating frame, and applications to orbit determination. Wright [33] adds air drag to Wiesel's solution to the Vinti problem by applying general perturbations techniques to the action-angle variables developed by Wiesel. Other related work by Biscani and Izzo [6] presented a complete solution to the Euler problem or problem of two fixed centers, whose connection to the Vinti problem has been known for some time [8]. The Euler problem is considered a stepping stone between the two-body problem and the circular restricted three-body problem, and is equally applicable to modeling the orbital dynamics around rotationally symmetric primary bodies. The solution of Biscani and Izzo [6] applies to bounded and unbounded orbits of objects under attractive or repulsive forces.

Recent work on Vinti theory by the present authors began in 2016 when it was revisited in a relative motion context [2, 5], employing the asymmetric Vinti potential that is fit to the  $J_2$  and  $J_3$  spherical harmonic coefficients of a celestial body [27, 28].

---

<sup>1</sup>Information on GTOC 9 can be accessed at this website: [https://sophia.estec.esa.int/gtoc\\_portal/?page\\_id=814](https://sophia.estec.esa.int/gtoc_portal/?page_id=814)

The work improved somewhat on Vinti theory itself, addressing computational questions, singularities, and numerical problems in the domain of bounded orbits. The removal of a number of numerical issues generally brought the theory to a level commensurate with methods for propagating classical spherical elements with two-body dynamics in the same domain and transforming between those coordinates and inertial position and velocity. The solution was implemented to order  $O(J_2^4)$  in the secular terms and  $O(J_2^2)$  in the periodic terms, and while it is adjustable to higher order, it is presently an approximate solution to the Vinti problem and does not possess double-precision accuracy. This solution can, in principle, be extended to an order sufficient for double-precision accuracy without elliptic functions as long as  $J_2$  is less than roughly 0.17, when the series expansions are valid [14, 25].

The investigation [2, 5] also established the structure of the fundamental state transition matrix (STM) in the classical spheroidal element space. While the structure is fixed, the authors developed its components in a two-part piecewise fashion to eliminate singularities in the partial derivatives. What the authors did not address is the issue of linear dependence that can arise between the columns of the STM when the bookend transformations to and from Earth-centered inertial (ECI) coordinates are included. This issue should not come as a surprise because the exact same phenomenon arises for classical spherical elements. To remove the linear dependence for all combinations of spheroidal eccentricity and inclination, the effort continued with the development of a nonsingular element set: the oblate spheroidal equinoctial orbital elements [3, 4]. These elements employ the symmetric Vinti potential because shifting the origin of the oblate spheroidal (OS) reference frame to account for  $J_3$  hamstrings the definition of an equinoctial element set [4]. In choosing the symmetric gravitational potential, oblateness of the primary is embedded in the coordinates.

The complete introduction of the spheroidal equinoctial orbital elements is divided into two parts. The first study [3] generalized the standard, spherical equinoctial orbital elements [7, 11] to an oblate spheroidal geometry congruent with Vinti theory. The effort focused on developing the point transformations that map between the equinoctial elements and the inertial position and velocity vectors, including derivations and algorithms. Their function, as such, is akin to that of the transformations established for spherical elements, wherein notions of osculating elements can be adopted for a perturbed Vinti problem. State propagation in time is viewed as a separate problem, and the analytical treatment is the subject of the present work.

The approach to analytical state propagation proceeds in the spirit of Vinti [24, 29], reducing the inversion of the kinematic equations to successive solutions of Kepler's equation, modified here for equinoctial elements. Other techniques have been suggested for the inversion expressed in classical elements [34]; the approach here can exploit iterative root-solve algorithms typical for solving Kepler's equation. The authors recommend Laguerre's method modified from Conway's form [10] because of the robustness it affords in the form of a free parameter that controls the order of the root-solve. Der [13] employs this method for the same reason. To reach this stage of the solution, many smaller steps must be taken, which are outlined here. First, Vinti's kinematic equations are re-expressed in spheroidal equinoctial elements. The secular terms of the solution are transformed first, followed by the periodic terms. Next, the spheroidal equinoctial integrals of the motion are derived. Like the classical

element solution, these integrals of the motion are based on the spheroidal Delaunay variables that Vinti employed. These Delaunay variables enable the extraction of the periodic components of the equinoctial elements, which in turn make the equinoctial integrals of the motion accessible. These latter elements are easily propagated in time, and after the described root-solve, the final goal is obtained: an analytical solution to the Vinti problem in equinoctial elements. The investigation concludes with a number of examples to test the analytical Vinti orbit propagator.

## Problem Statement

Vinti's analytical solution can be expressed as a nonlinear function  $\mathbf{f}$  of the initial state  $\mathbf{x}_i$ . More precisely, the solution can be written as

$$\mathbf{x} = \mathbf{f}(t, \mathbf{x}_i), \quad (1)$$

where the state vector is defined as

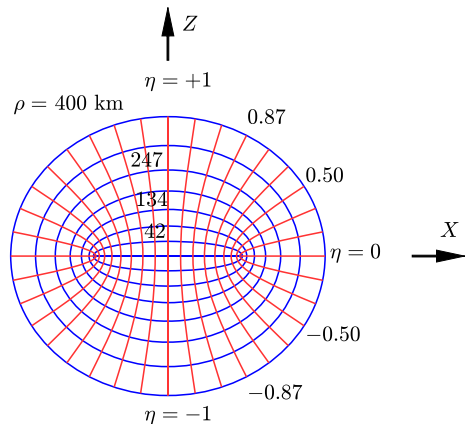
$$\mathbf{x}^\top = [\mathbf{r}^\top \ \mathbf{v}^\top], \quad (2)$$

so that in ECI coordinates,  $\mathbf{x} = [X, Y, Z, \dot{X}, \dot{Y}, \dot{Z}]^\top$ . The quantities  $\mathbf{r}$  and  $\mathbf{v}$  represent inertial position and velocity vectors, respectively. The dynamical problem considered concerns a spacecraft traveling under the influence of the symmetric Vinti potential [23]

$$V = -\frac{\mu\rho}{\rho^2 + c^2\eta^2}, \quad (3)$$

where  $\mu = GM$  is the gravitational parameter of the primary,  $\rho$  is the OS coordinate equal to the semiminor axis of the tangent oblate spheroid,  $\eta$  is the OS coordinate associated with latitude that is approximately equal to the sine of the declination, and  $2c$  is the focal separation for the oblate spheroid ( $c$  is the radius of the oblate spheroid's focal circle). The OS coordinate system geometry is illustrated in Fig. 1, which presents a cross-section of the  $XZ$ -plane. The third OS coordinate is the right ascension,  $\phi$ , which is identical to the azimuthal angle in spherical coordinates. The

**Fig. 1** Geometry of oblate spheroidal coordinates for Earth: cross-section of the  $XZ$ -plane (the  $\eta = 0$  line marks the equatorial plane) zoomed in to an equatorial radius of approximately 451 km [5]



ECI and OS reference frames share the same origin. Constant values of  $\rho$  specify confocal oblate spheroids, those of  $\eta$  specify confocal hyperboloids of one sheet, and those of  $\phi$  specify meridional planes. The focal separation is fit to the dominant term of the traditional spherical harmonic potential as

$$c^2 = R_e^2 J_2, \tag{4}$$

where  $R_e$  is the equatorial radius. With this fit, the Vinti potential is exact for a symmetric oblate spheroid where  $J_4 = -J_2^2$ ,  $J_6 = +J_2^3$ ,  $\dots$ , but relative to the Earth’s potential, for example, the fit is approximate, notionally modeling  $J_2 + \epsilon J_4 + \epsilon^2 J_6 + \dots$  for some small  $\epsilon$ . In the case of the Earth, the Vinti potential includes roughly 72% of  $J_4$ .

Using the gravitational potential  $V$  of Eq. 3 and OS coordinates, Vinti derived the Hamiltonian,  $\mathcal{H}$ , as

$$\mathcal{H} = \frac{1}{2} \left[ \frac{\rho^2 + c^2}{\rho^2 + c^2 \eta^2} p_\rho^2 + \frac{1 - \eta^2}{\rho^2 + c^2 \eta^2} p_\eta^2 + \frac{1}{(\rho^2 + c^2)(1 - \eta^2)} p_\phi^2 \right] - \frac{\mu\rho}{\rho^2 + c^2 \eta^2}, \tag{5}$$

where  $p_\rho$ ,  $p_\eta$ , and  $p_\phi$  are the conjugate momenta given by

$$p_\rho = \frac{\rho^2 + c^2 \eta^2}{\rho^2 + c^2} \dot{\rho} \tag{6}$$

$$p_\eta = \frac{\rho^2 + c^2 \eta^2}{1 - \eta^2} \dot{\eta} \tag{7}$$

$$p_\phi = (\rho^2 + c^2) (1 - \eta^2) \dot{\phi}. \tag{8}$$

He then solved the dynamical problem by obtaining the Hamilton-Jacobi equation and applying separation of variables [23].

Details on the notation and computation of certain constants and intermediate quantities are available in a number of references [24, 27, 29] and are not covered in this paper. Corrections to certain quantities, such as the  $B_j$  and  $B_{jk}$  coefficients, are given in Walden and Watson [30]. The notation in this paper follows the notation of Vinti’s 1966 theory [27] except that  $J_3$  is set to zero. Also note the use of the RAAN-like variable  $\Omega'$  that Vinti developed in 1969 [29].

### Kinematic Equations

Following the methods of Hamilton-Jacobi theory, the problem is reduced to a set of kinematic equations that define three of the six constants of the motion. The kinematic equations are generally expressed as [14]

$$t + \beta_1 = R_1 + c^2 N_1 \tag{9}$$

$$\beta_2 = -\alpha_2 R_2 + \alpha_2 N_2 \tag{10}$$

$$\beta_3 = \phi + c^2 \alpha_3 R_3 - \alpha_3 N_3, \tag{11}$$

where  $t$  denotes the time,  $R_j$  denotes the  $\rho$ -integrals for  $j = 1, 2, 3$  defined as

$$R_1 = \int_{\rho_1}^{\rho} \pm \rho^2 F(\rho)^{-1/2} d\rho \quad (12)$$

$$R_2 = \int_{\rho_1}^{\rho} \pm F(\rho)^{-1/2} d\rho \quad (13)$$

$$R_3 = \int_{\rho_1}^{\rho} \pm (\rho^2 + c^2)^{-1} F(\rho)^{-1/2} d\rho, \quad (14)$$

$N_j$  denotes the  $\eta$ -integrals for  $j = 1, 2, 3$  defined as

$$N_1 = \int_0^{\eta} \pm \eta^2 G(\eta)^{-1/2} d\eta \quad (15)$$

$$N_2 = \int_0^{\eta} \pm G(\eta)^{-1/2} d\eta \quad (16)$$

$$N_3 = \int_0^{\eta} \pm (1 - \eta^2)^{-1} G(\eta)^{-1/2} d\eta, \quad (17)$$

and  $\alpha_j$  and  $\beta_j$  are the Jacobi constants for  $j = 1, 2, 3$ . Specifically,  $\alpha_1$  is the total energy or Hamiltonian,  $\alpha_2$  is closely related to the total angular momentum,  $\alpha_3$  is the polar component of the angular momentum,  $\tau = -\beta_1$  is the time of spheroidal periapsis passage,  $\beta_2 = \omega$  is the argument of spheroidal periapsis, and  $\beta_3 = \Omega$  is the right ascension of the spheroidal ascending node (spheroidal RAAN). These six quantities are canonical constants of the motion analogous to the Jacobi constants obtained for the two-body problem. The quantities  $F(\rho)$  and  $G(\eta)$  correspond to the quartics that must be factored to obtain  $a$ ,  $e$ , and  $I$ , which are respectively the spheroidal semimajor axis, eccentricity, and inclination. For readability, the ‘‘spheroidal’’ qualifier is often omitted and elements should be understood as spheroidal unless noted otherwise.

The derivation of the approximate analytical solution in OS equinoctial elements begins with Vinti’s solution in classical elements. His classical element solution expressed Eqs. 9–11 correct to  $O(J_2^3)$  in secular terms and  $O(J_2^2)$  in periodic terms using truncated series as

$$t + \beta_1 = (-2\alpha_1)^{-1/2} \left[ b_1 E + a(E - e \sin E) + A_1 f + \sum_{k=1}^2 A_{1k} \sin kf \right] \\ + c^2 \alpha_2^{-1} u^{1/2} (B'_1 \psi + B_{12} \sin 2\psi + B_{14} \sin 4\psi) \quad (18)$$

$$\beta_2 = -\alpha_2 (-2\alpha_1)^{-1/2} \left[ A_2 f + \sum_{k=1}^4 A_{2k} \sin kf \right] \\ + u^{1/2} (B_2 \psi + B_{22} \sin 2\psi + B_{24} \sin 4\psi) \quad (19)$$

$$\beta_3 = \Omega' + c^2 \alpha_3 (-2\alpha_1)^{-1/2} \left[ A_3 f + \sum_{k=1}^4 A_{3k} \sin kf \right] \\ - \alpha_3 \alpha_2^{-1} u^{1/2} (B_3 \psi + B_{32} \sin 2\psi). \quad (20)$$

Readers can identify the familiar  $E - e \sin E$  term of the Kepler problem in Eq. 20 and view its appearance here as part of a generalized Kepler’s equation. The variable  $f$  is the spheroidal true anomaly,  $E$  is the spheroidal eccentric anomaly, and  $\psi$  is the true argument of spheroidal latitude. The quantities  $b_1, A_j, A_{jk}, B_j, B_{jk}$ , and  $u$  are constants. When using Vinti’s method of computing  $u$ , the solution is accurate to  $O(J_2^3)$  in secular terms, as stated. However, as presently implemented,  $u$  is computed from Getchell’s factorization algorithm to arbitrary accuracy [17], ultimately making the solution accurate to  $O(J_2^4)$  in secular terms [27].

**Definition of Oblate Spheroidal Equinoctial Orbital Elements**

As stated earlier, details on the coordinate transformation between ECI coordinates and OS equinoctial elements are located in a separate paper by the authors [3]. The six modified OS equinoctial elements are described as follows using the notation of Gim and Alfriend [18] for the vector components<sup>2</sup>

$$\begin{aligned}
 \alpha_1 &= p && \text{spheroidal semilatus rectum} \\
 \alpha_2 &= q_1 \\
 \alpha_3 &= q_2 && \left. \begin{array}{l} \alpha_2 = q_1 \\ \alpha_3 = q_2 \end{array} \right\} \text{components of the spheroidal eccentricity vector} \\
 \alpha_4 &= p_1 \\
 \alpha_5 &= p_2 && \left. \begin{array}{l} \alpha_4 = p_1 \\ \alpha_5 = p_2 \end{array} \right\} \text{components of the spheroidal ascending node vector} \\
 \alpha_6 &= L && \text{true spheroidal longitude}
 \end{aligned} \tag{21}$$

Walker et al. [31] coined the terminology that distinguishes between standard and modified equinoctial elements, where the standard OS equinoctial elements would use semimajor axis  $a$  instead of  $p$  and the mean spheroidal longitude  $\lambda$  instead of  $L$ . The modified set is chosen because it is nonsingular for the full range of eccentricity and inclination. The definition of equinoctial elements in terms of classical elements is repeated here for convenience. Given OS classical elements, the OS equinoctial elements are determined as

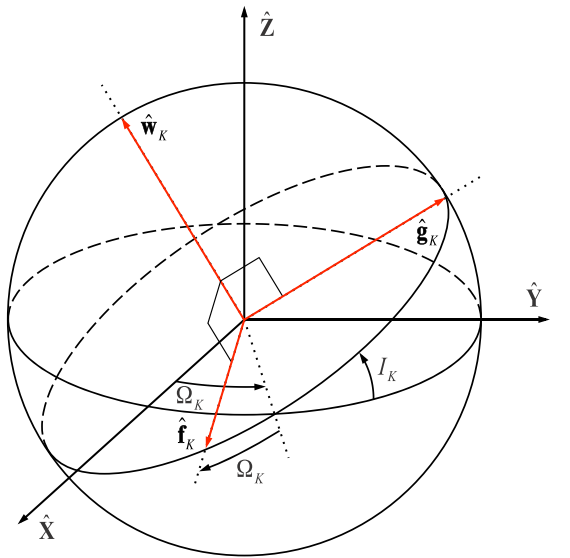
$$\begin{aligned}
 p &= p \\
 q_1 &= e \cos (\omega' + K \Omega') \\
 q_2 &= e \sin (\omega' + K \Omega') \\
 p_1 &= \left[ \tan \left( \frac{I}{2} \right) \right]^K \cos \Omega' \\
 p_2 &= \left[ \tan \left( \frac{I}{2} \right) \right]^K \sin \Omega' \\
 L &= f + \omega' + K \Omega',
 \end{aligned} \tag{22}$$

<sup>2</sup>In the work of Gim and Alfriend, the spherical orbital elements are used to define a curvilinear coordinate system.

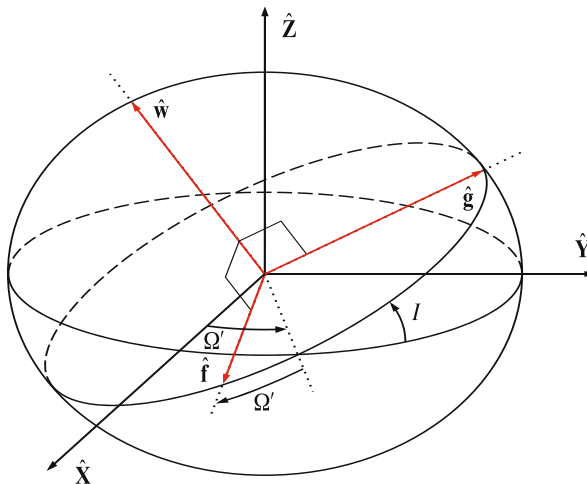
where  $\psi = f + \omega'$ ,  $K$  is the retrograde factor defined as

$$K = \begin{cases} +1 & \text{direct OS equinoctial elements} \\ -1 & \text{retrograde OS equinoctial elements} \end{cases}, \quad (23)$$

$\Omega'$  is a different RAAN, and  $\omega'$  is a different argument of periapsis. The ' symbol distinguishes these variables from the constants of the motion  $\beta_2 = \omega$  and  $\beta_3 = \Omega$  and also indicates a closer connection to the spheroidal Delaunay variables obtained after



(a) Spherical geometry (Keplerian elements)



(b) Oblate spheroidal geometry (non-Keplerian elements)

**Fig. 2** Direct equinoctial reference frames for different geometries [4]



various canonical transformations. The connection between these angular variables and the associated constants will be made clear in subsequent sections with explicit equations. For clarity, the direct equinoctial reference frames associated with spherical and spheroidal geometry are respectively illustrated side by side in Fig. 2a and b.

While the constants of the motion are important, the solution method presented in this work, which builds on Vinti’s classical element approach, utilizes the spheroidal Delaunay variables to solve the Vinti problem. To see why, consider a simple analogy. In the Kepler problem, a solution is obtained in terms of the mean anomaly and not the corresponding constant of the motion, the time of periapsis passage. In the Vinti problem, the spheroidal RAAN and argument of periapsis constants must similarly be transformed to spheroidal Delaunay variables in order to solve the problem in this manner.

### Converting to Equinoctial Elements: Secular Terms

Writing the secular components in terms of equinoctial elements requires the following definition for eccentric spheroidal longitude,  $F$ :

$$F = E + \omega' + K\Omega' \tag{24}$$

It is also convenient at this time to similarly define the mean spheroidal longitude as

$$\lambda = M + \omega' + K\Omega', \tag{25}$$

where  $M$  denotes the spheroidal mean anomaly.

From Eqs. 22 and 24, observe that certain combinations of angles must be added to both sides of Eqs. 18–20 to obtain  $L$  and  $F$  on the right-hand side (RHS). First, focus on Eq. 18 and consider the term  $(a + b_1)E$ . Adding  $(-2\alpha_1)^{-1/2} (a + b_1)(\omega' + K\Omega')$  to both sides will result in a  $(a + b_1)F$  term on the RHS and the left-hand side (LHS) can simply absorb the unknown quantity into the unknown constant  $\beta_1$ . The new quantities on the LHS are denoted as  $\tilde{\beta}_j$  for  $j = 1, 2, 3$ . This procedure is generally applied to the remaining secular terms in Eqs. 18–20, resulting in the following transformed equations:

$$t + \tilde{\beta}_1 = (-2\alpha_1)^{-1/2} \left[ b_1 F + a (F - e \sin E) + A_1 L + \sum_{k=1}^2 A_{1k} \sin kf \right] + c^2 \alpha_2^{-1} u^{1/2} (B'_1 L + B_{12} \sin 2\psi + B_{14} \sin 4\psi) \tag{26}$$

$$\tilde{\beta}_2 \alpha_2^{-1} = -(-2\alpha_1)^{-1/2} \left[ A_2 L + \sum_{k=1}^4 A_{2k} \sin kf \right] + \alpha_2^{-1} u^{1/2} (B_2 L + B_{22} \sin 2\psi + B_{24} \sin 4\psi) \tag{27}$$

$$\tilde{\beta}_3 = c^2 \alpha_3 (-2\alpha_1)^{-1/2} \left[ A_3 L + \sum_{k=1}^4 A_{3k} \sin kf \right] - \alpha_3 \alpha_2^{-1} u^{1/2} (B_3 L + B_{32} \sin 2\psi), \tag{28}$$

where

$$\begin{aligned} \tilde{\beta}_1 &= \beta_1 + (-2\alpha_1)^{-1/2} (a + b_1 + A_1)(\omega' + K\Omega') + c^2\alpha_2^{-1}u^{1/2}B'_1K\Omega' \quad (29) \\ \tilde{\beta}_2\alpha_2^{-1} &= \beta_2\alpha_2^{-1} - (-2\alpha_1)^{-1/2} A_2(\omega' + K\Omega') + \alpha_2^{-1}u^{1/2}B_2K\Omega' \quad (30) \\ \tilde{\beta}_3 &= \beta_3 + c^2\alpha_3(-2\alpha_1)^{-1/2} A_3(\omega' + K\Omega') \\ &\quad - \alpha_3\alpha_2^{-1}u^{1/2}B_3K\Omega' - \Omega'. \quad (31) \end{aligned}$$

Equations 29–31 are an important intermediate result that will be useful later, but the transformation is not yet complete because the periodic terms, having not been addressed, still contain  $f$  and  $\psi$ .

### Converting to Equinoctial Elements: Periodic Terms

There are multiple ways to proceed, but the approach here aims to maintain the form of the periodic terms where the sines contain multiple-angle arguments of  $kf$  or  $k\psi$  for  $k = 1, \dots, 4$ . These trigonometric terms can be written in terms of equinoctial elements by applying Chebyshev’s recursive formula and observing that the periodic coefficients  $A_{jk}$  contain a factor  $e^k$  and  $B_{jk}$  contain a factor  $Q^k$ , where  $j = 1, 2, 3$  denotes the kinematic equation and  $k = 1, \dots, 4$ . Define new periodic coefficients in terms of the old as

$$\tilde{A}_{jk} \equiv \frac{A_{jk}}{e^k} \quad (32)$$

$$\tilde{B}_{jk} \equiv \frac{B_{jk}}{Q^k}. \quad (33)$$

Note that the new coefficients should not be computed this way since  $e$  and/or  $Q$  can go to zero, where  $Q = \sin I'$  and  $I' = I$  when  $J_3 = 0$ . To compute  $\tilde{A}_{jk}$  or  $\tilde{B}_{jk}$ , simply use the original formulas with omission of  $e^k$  and  $Q^k$ . Now,  $e^k$  and  $Q^k$  are instead grouped with the sine functions, such as  $e \sin f$  or  $Q^4 \sin 4\psi$ .

The basic conversion process is demonstrated for the  $e \sin E$  term. It is straightforward to show from angle sum and difference identities that

$$\begin{aligned} e \sin E &= e \sin (F - \omega' - K\Omega') \\ &= e \sin F \cos (\omega' + K\Omega') - e \cos F \sin (\omega' + K\Omega'). \quad (34) \end{aligned}$$

Therefore,

$$e \sin E = q_1 \sin F - q_2 \cos F. \quad (35)$$

Applying similar identities for  $e \cos E$  gives

$$e \cos E = q_1 \cos F + q_2 \sin F. \quad (36)$$

This process can be applied recursively for any argument  $x$  and for all terms of higher frequency using Chebyshev’s formula,

$$\sin nx = 2 \cos x \sin [(n - 1)x] - \sin [(n - 2)x], \quad (37)$$

for a positive integer  $n \geq 2$ . For example, with  $n = 2$ ,  $e^2 \sin 2f = 2e^2 \cos f \sin f$  can be grouped in terms of lower-frequency quantities as  $2(e \cos f)(e \sin f)$ . Carrying

out the process to the fourth term gives the following relations for periodic functions of  $kf$  in terms of periodic functions of  $kL$ :

$$\tilde{q}_1(q_1, q_2, L) \equiv e \sin f = q_1 \sin L - q_2 \cos L \tag{38}$$

$$\tilde{q}_2(q_1, q_2, L) \equiv e^2 \sin 2f = (q_1^2 - q_2^2) \sin 2L - 2q_1q_2 \cos 2L \tag{39}$$

$$\tilde{q}_3(q_1, q_2, L) \equiv e^3 \sin 3f = (q_1^3 - q_1q_2^2) \sin 3L + (q_2^3 - q_1^2q_2) \cos 3L \tag{40}$$

$$\begin{aligned} \tilde{q}_4(q_1, q_2, L) \equiv e^4 \sin 4f = & (q_1^4 - 6q_1^2q_2^2 + q_2^4) \sin 4L \\ & + 4(q_1q_2^3 - q_1^3q_2) \cos 4L. \end{aligned} \tag{41}$$

The periodic functions of  $k\psi$  in terms of periodic functions of  $kL$  are slightly more complicated to derive. The form of these relations is identical to that of the relations for  $kf$  except that there is now a coefficient  $(1 + K \cos I)^k$ . The relations are stated as

$$\begin{aligned} \tilde{p}_2(p_1, p_2, L) \equiv Q^2 \sin 2\psi = & (1 + K \cos I)^2 \left[ (p_1^2 - p_2^2) \sin 2L \right. \\ & \left. - 2Kp_1p_2 \cos 2L \right] \end{aligned} \tag{42}$$

$$\begin{aligned} \tilde{p}_4(p_1, p_2, L) \equiv Q^4 \sin 4\psi = & (1 + K \cos I)^4 \left[ (p_1^4 - 6p_1^2p_2^2 + p_2^4) \sin 4L \right. \\ & \left. + 4K(p_1p_2^3 - p_1^3p_2) \cos 4L \right]. \end{aligned} \tag{43}$$

These equations can be written strictly in terms of  $p_1$  and  $p_2$  by observing that

$$\begin{aligned} (1 + K \cos I)^2 &= \frac{4}{4} (1 + K \cos I)^2 \\ &= 4 \left( \frac{1 + K \cos I}{2} \right)^2 \\ &= \begin{cases} 4 \cos^4 \left( \frac{I}{2} \right), & \text{if } K = +1 \\ 4 \sin^4 \left( \frac{I}{2} \right), & \text{if } K = -1 \end{cases} \end{aligned} \tag{44}$$

It follows that

$$(1 + K \cos I)^2 = \frac{4}{(1 + p_1^2 + p_2^2)^2} \tag{45}$$

for either value of  $K$ . Eq. 45 can be substituted into Eq. 42. Squaring Eq. 45 gives

$$(1 + K \cos I)^4 = \frac{16}{(1 + p_1^2 + p_2^2)^4}, \tag{46}$$

which can be substituted into Eq. 43. After the substitutions, Eqs. 42 and 43 become

$$Q^2 \sin 2\psi = \frac{4}{(1 + p_1^2 + p_2^2)^2} \left[ (p_1^2 - p_2^2) \sin 2L - 2Kp_1p_2 \cos 2L \right] \tag{47}$$

$$\begin{aligned} Q^4 \sin 4\psi = & \frac{16}{(1 + p_1^2 + p_2^2)^4} \left[ (p_1^4 - 6p_1^2p_2^2 + p_2^4) \sin 4L \right. \\ & \left. + 4K(p_1p_2^3 - p_1^3p_2) \cos 4L \right]. \end{aligned} \tag{48}$$

## Converting to Equinoctial Elements: Final Kinematic Equations

Finally, having represented the secular and periodic terms with spheroidal equinoctial elements, the kinematic equations can be expressed strictly in terms of these nonsingular orbital elements as

$$t + \tilde{\beta}_1 = (-2\alpha_1)^{-1/2} \left[ b_1 F + a (F - q_1 \sin F + q_2 \cos F) + A_1 L + \sum_{k=1}^2 \tilde{A}_{1k} e^k \sin kf \right] + c^2 \alpha_2^{-1} u^{1/2} \left( B'_1 L + \tilde{B}_{12} Q^2 \sin 2\psi + \tilde{B}_{14} Q^4 \sin 4\psi \right) \quad (49)$$

$$\tilde{\beta}_2 \alpha_2^{-1} = -(-2\alpha_1)^{-1/2} \left[ A_2 L + \sum_{k=1}^4 \tilde{A}_{2k} e^k \sin kf \right] + \alpha_2^{-1} u^{1/2} \left( B_2 L + \tilde{B}_{22} Q^2 \sin 2\psi + \tilde{B}_{24} Q^4 \sin 4\psi \right) \quad (50)$$

$$\tilde{\beta}_3 = c^2 \alpha_3 (-2\alpha_1)^{-1/2} \left[ A_3 L + \sum_{k=1}^4 \tilde{A}_{3k} e^k \sin kf \right] - \alpha_3 \alpha_2^{-1} u^{1/2} \left( B_3 L + \tilde{B}_{32} Q^2 \sin 2\psi \right), \quad (51)$$

where it is understood that Eqs. 38–41 and 47–48 can be substituted for the periodic terms in  $e^k \sin kf$  and  $Q^k \sin k\psi$ . The substitution is useful for the propagation step, but not essential for the present coordinate transformation. The reason is that, while  $\sin f$  and  $\sin \psi$  are undefined for the singular cases, nonsingular expressions do exist for  $e \sin f$  and  $Q \sin \psi$ . For this particular coordinate transformation, it is more computationally efficient to combine these latter expressions with Chebyshev's formula in Eq. 37 than to use the more complicated equinoctial form. When computing the elements from initial conditions in ECI coordinates at an initial time  $t_i$ , the right-hand sides of Eqs. 49–51 are calculable.

## Equinoctial Integrals of the Motion and Spheroidal Delaunay Variables

It is instructive to first give a motivation of why oblate spheroidal equinoctial integrals of the motion are desired and a road map of how to obtain them.

### Motivation

As emphasized in Biria and Russell [3], there is a notion of complete elements associated with the angular variables,  $\Omega'$ ,  $\omega'$ , and  $f$  (and combinations thereof), which are

viewed as the composition of secular and periodic parts, expressed mathematically as

$$\Omega' = \Omega'_s + \Omega'_p \tag{52}$$

$$\omega' = \omega'_s + \omega'_p \tag{53}$$

$$f = M_s + f_p. \tag{54}$$

The subscript “s” denotes a secular part and the subscript “p” denotes a periodic part. If the initial values of the secular parts of the spheroidal equinoctial elements are available, then their linear dependence on time facilitates their propagation. The periodic parts can be added later in concert with solving the generalized Kepler’s equation. These initial values may be given somehow, but if they must be obtained from initial ECI coordinates, then the following discussion and derivations apply.

### A Road Map to Obtaining the OS Equinoctial Integrals of the Motion

The work of Biria and Russell [3] demonstrated how to obtain the complete equinoctial orbital elements  $\{p, q_1, q_2, p_1, p_2, L\}$  from ECI coordinates. Applying angle sum identities to the definitions of  $q_1$  and  $q_2$  in Eq. 22 after separating the angles into secular and periodic parts as

$$q_1 = e \cos(\omega' + K\Omega') = e \cos(\omega'_s + K\Omega'_s + \omega'_p + K\Omega'_p) \tag{55}$$

$$q_2 = e \sin(\omega' + K\Omega') = e \sin(\omega'_s + K\Omega'_s + \omega'_p + K\Omega'_p) \tag{56}$$

gives

$$q_1 = q_{1s} \cos(\omega'_p + K\Omega'_p) - q_{2s} \sin(\omega'_p + K\Omega'_p) \tag{57}$$

$$q_2 = q_{1s} \sin(\omega'_p + K\Omega'_p) + q_{2s} \cos(\omega'_p + K\Omega'_p), \tag{58}$$

and inverting the equations to solve for  $q_{js}$  gives

$$\begin{bmatrix} q_{1s} \\ q_{2s} \end{bmatrix} = \begin{bmatrix} \cos(\omega'_p + K\Omega'_p) & \sin(\omega'_p + K\Omega'_p) \\ -\sin(\omega'_p + K\Omega'_p) & \cos(\omega'_p + K\Omega'_p) \end{bmatrix} \begin{bmatrix} q_1 \\ q_2 \end{bmatrix}. \tag{59}$$

Equation 59 indicates that the secular parts of  $q_1$  and  $q_2$  are calculable as long as the periodic parts of  $\omega'$  and  $\Omega'$  are known. Similarly, the elements  $p_{js}$  are determined as

$$\begin{bmatrix} p_{1s} \\ p_{2s} \end{bmatrix} = \begin{bmatrix} \cos \Omega'_p & \sin \Omega'_p \\ -\sin \Omega'_p & \cos \Omega'_p \end{bmatrix} \begin{bmatrix} p_1 \\ p_2 \end{bmatrix}. \tag{60}$$

Lastly, the secular part of the true longitude,  $L_s = M_s + \omega'_s + K\Omega'_s$ , is also desired. Note that  $L_s$  is equivalent to the secular part of the mean longitude,  $\lambda_s$ . As shown in the following, it turns out that  $\lambda_s$  can be obtained directly. Therefore, the unknowns to be solved for in the following derivation are  $\omega'_p, \Omega'_p$ , and  $\lambda_s$ .

## Oblate Spheroidal Delaunay Elements

The oblate spheroidal equinoctial integrals of the motion are obtained from the spheroidal Delaunay elements that Vinti employed for his perturbation work [26]. Vinti partly attributes these elements to Izsak [19]. The spheroidal Delaunay variables describe the secular evolution of a Vinti trajectory and are the result of several canonical transformations. While not always clear in the literature, it is important to note that the secular components of certain spheroidal orbital elements are equivalent to the Delaunay elements. Using the subscript “s” to indicate that the quantity only contains the secular part, the relations are given by

$$l \equiv M_s \quad (61)$$

$$g \equiv \omega'_s \quad (62)$$

$$h \equiv \Omega'_s. \quad (63)$$

Adopting Delaunay’s notation serves as a helpful reminder that these are canonical elements. However, it is emphasized that the elements  $M$ ,  $\omega'$ , and  $\Omega'$  are not canonical when the periodic components are included. This feature is distinctly different from the two-body problem, wherein the mean anomaly is canonical and simply varies linearly with time. Interestingly, the relation  $\Omega'_s = h$  was not pointed out until 1980 [34] and the relation  $\omega'_s = g$  has never been given explicitly.

Next, the evolution of the spheroidal Delaunay variables must be described explicitly. Their values at  $t = 0$  are given in terms of the original canonical elements as

$$l_0 = 2\pi v_1 \left( \beta_1 - c^2 \beta_2 \alpha_2^{-1} B'_1 B_2^{-1} \right) \quad (64)$$

$$l_0 + g_0 = 2\pi v_2 \left[ \beta_1 + \beta_2 \alpha_2^{-1} (a + b_1 + A_1) A_2^{-1} \right] \quad (65)$$

$$h_0 = \beta_3 - c^2 \alpha_3 (-2\alpha_1)^{-1/2} A_3 l_0 + \alpha_3 \alpha_2^{-1} u^{1/2} B_3 (l_0 + g_0), \quad (66)$$

where the  $v_j$  are the fundamental frequencies, later defined explicitly. Eqs. 64 and 65 are given by Vinti [27] and Eq. 66 can be interpreted from Eq. (9) in Wu and Tong [34]. Before moving on, observe in Eqs. 64–66 that  $l_0$  and  $h_0$  are easily isolated but not  $g_0$ . While  $g_0$  could be isolated and an expression for it obtained, as formulated,  $g_0$  always appears with  $l_0$  as  $l_0 + g_0$ . It is therefore useful to draw one more connection between the OS elements and the Delaunay elements. The equivalence between the secular part of the true argument of spheroidal latitude and the sum of two of the Delaunay elements can be stated as

$$\psi_s \equiv l + g. \quad (67)$$

Now, naturally, the relations in Eqs. 64–66 still hold, as the dynamical problem is unchanged. These Delaunay elements are not calculable when seeking nonsingular elements because the  $\beta_j$  are unknown, but Eqs. 64–66 will still be of great use. To

see how, notice that the  $\tilde{\beta}_j$  are known and Eqs. 29–31 can be used to substitute for  $\beta_j$  in Eqs. 64–66. Note that while Vinti preferred to maintain  $\beta_3$  as an element in his classical element solution, this luxury is no longer available because the third kinematic equation is no longer decoupled from the others in an equinoctial element solution. The spheroidal Delaunay element  $h_0$  must then be used instead of  $\beta_3$ , as will be seen shortly.

Substituting Eqs. 29–31 for  $\beta_j$  in Eqs. 64–66 and simplifying leads to the following simple equations

$$l_0 + \omega'_i + K\Omega'_i = 2\pi v_1 \left( \tilde{\beta}_1 - c^2 \tilde{\beta}_2 \alpha_2^{-1} B'_1 B_2^{-1} \right) \tag{68}$$

$$l_0 + g_0 + K\Omega'_i = 2\pi v_2 \left[ \tilde{\beta}_1 + \tilde{\beta}_2 \alpha_2^{-1} (a + b_1 + A_1) A_2^{-1} \right] \tag{69}$$

$$h_0 - \Omega'_i = \tilde{\beta}_3 - c^2 \alpha_3 (-2\alpha_1)^{-1/2} A_3 (l_0 + \omega'_i + K\Omega'_i) + \alpha_3 \alpha_2^{-1} u^{1/2} B_3 (l_0 + g_0 + K\Omega'_i). \tag{70}$$

The right-hand sides of Eqs. 68–70 are identical in form to Eqs. 64–66, but  $\beta_j$  is replaced by  $\tilde{\beta}_j$ , making the right-hand sides calculable. Notice on the left-hand sides of Eqs. 68–70 that the elements are referenced to different epochs. The spheroidal Delaunay elements correspond to the time  $t = 0$ , denoted by subscript “0”, while the classical spheroidal elements reference some given initial time, denoted by subscript “i”.

To reconcile these differences in epoch, the Delaunay elements are adjusted to reference the same given initial time. Vinti wrote the secular evolution of these elements referenced to the time  $t = 0$  as

$$l = l_0 + 2\pi v_1 t \tag{71}$$

$$l + g = l_0 + g_0 + 2\pi v_2 t \tag{72}$$

$$h = h_0 + 2\pi (v_3 - v_2 \operatorname{sgn} \alpha_3) t, \tag{73}$$

but these dynamics can be equivalently referenced to a given initial time (or arbitrary time) as

$$l = l_i + 2\pi v_1 (t - t_i) \tag{74}$$

$$l + g = l_i + g_i + 2\pi v_2 (t - t_i) \tag{75}$$

$$h = h_i + 2\pi (v_3 - v_2 \operatorname{sgn} \alpha_3) (t - t_i), \tag{76}$$

where

$$l_i = l_0 + 2\pi v_1 t_i \tag{77}$$

$$l_i + g_i = l_0 + g_0 + 2\pi v_2 t_i \tag{78}$$

$$h_i = h_0 + 2\pi (v_3 - v_2 \operatorname{sgn} \alpha_3) t_i. \tag{79}$$

For convenience, the constant fundamental frequencies  $\nu_j$  are given below as

$$\dot{M}_s = 2\pi\nu_1 = \frac{(-2\alpha_1)^{1/2}}{a_0 + A_1 + c^2 A_2 B_1' B_2^{-1}} \quad (80)$$

$$\dot{\psi}_s = 2\pi\nu_2 = \frac{\alpha_2 u^{-1/2} A_2 B_2^{-1}}{a_0 + A_1 + c^2 A_2 B_1' B_2^{-1}} \quad (81)$$

$$\dot{\phi}_s = 2\pi\nu_3 = \frac{-\alpha_3}{a_0 + A_1 + c^2 A_2 B_1' B_2^{-1}} \times \left\{ c^2 A_3 - \frac{A_2}{B_2} \left[ B_3 + \frac{1}{\tilde{S}} \left( \frac{h_1}{\sqrt{1-2\zeta}} + \frac{h_2}{\sqrt{1+2\zeta}} \right) \right] \right\}, \quad (82)$$

where  $\tilde{S} = \sqrt{1-S}$ , and  $S = \sin^2 I$ ,  $h_1$ ,  $h_2$ , and  $\zeta$  are constants from Vinti's 1966 solution [27]. Equations 80 and 81 are derived by Vinti [27] and Eq. 82 is derived in Biria and Russell [5]. Note that  $\nu_3$  is composed of a linear combination of  $\nu_1$  and  $\nu_2$ , and is directly related to the secular motion of right ascension. Since right ascension is discontinuous for polar orbits and poorly defined for nearly polar orbits, observable in the division by  $\tilde{S}$ , an alternative variable or expression is required to make the theory uniformly valid.

### Removing the Polar Orbit Singularity

An aside is necessary here to address the removal of the singularity in Eq. 82. First, note that the time derivative of Eq. 73 is clearly determined as

$$\dot{h} = 2\pi (\nu_3 - \nu_2 \operatorname{sgn} \alpha_3). \quad (83)$$

Now, one option is to directly replace  $h$  by  $\Omega'_s$ , the secular part of a slowly-changing variable  $\Omega'$  similar to the Keplerian RAAN that tracks a slowly rotating reference plane [29], obtained by removing the part of  $\phi_s$  that varies rapidly near a pole. Upon removal of the fast part, Eq. 83 can be replaced by

$$\dot{h} = \dot{\Omega}'_s = -\frac{\alpha_3}{a_0 + A_1 + c^2 A_2 B_1' B_2^{-1}} \left( c^2 A_3 - \frac{A_2}{B_2} B_3 \right). \quad (84)$$

With some manipulation, it can be shown that this expression agrees with the derivative of Wu and Tong's formula [34] for  $\Omega'_s$ . The same result is obtained by ignoring the periodic terms in Vinti's full expression for  $\Omega'$  [29]. Further justification for removing the fast part is that the ECI coordinates can be expressed in terms of the elements in such a way that they do not depend on the fast part, only on  $\Omega'$ .

An alternative approach leading to the same result is to observe that since the present interest is in  $\dot{h}$ , an alternative expression for  $\dot{\phi}_s$  can be used that does not contain the singularity. By substituting Eqs. (27), (147), (149.1), and (154) from Vinti



[27] into Eq. 82 of this paper and manipulating the equations, it is possible to show that

$$\frac{\alpha_3}{\sqrt{1-S}} \left( \frac{h_1}{\sqrt{1-2\zeta}} + \frac{h_2}{\sqrt{1+2\zeta}} \right) = \frac{\alpha_2}{\sqrt{u}} \operatorname{sgn} \alpha_3, \tag{85}$$

where the  $\sqrt{1-S}$  in the denominator cancels with the term in  $\alpha_3$ . Making this substitution in Eq. 82, Eq. 83 can be readily applied to arrive at the expression in Eq. 84 for  $\dot{h} = \dot{\Omega}'_s$ .

**Final Nonsingular Equations for the Unknowns**

Finally, Eqs. 68–70 can be referenced to a consistent epoch (the given initial time) and the singularity associated with polar orbits can be removed. The final result is

$$l_i + \omega'_i + K \Omega'_i = 2\pi v_1 \left( t_i + \tilde{\beta}_1 - c^2 \tilde{\beta}_2 \alpha_2^{-1} B'_1 B_2^{-1} \right) \tag{86}$$

$$l_i + g_i + K \Omega'_i = 2\pi v_2 \left[ t_i + \tilde{\beta}_1 + \tilde{\beta}_2 \alpha_2^{-1} (a + b_1 + A_1) A_2^{-1} \right] \tag{87}$$

$$\begin{aligned} h_i - \Omega'_i = & \tilde{\beta}_3 + \dot{h} t_i \\ & - c^2 \frac{\alpha_3}{(-2\alpha_1)^{1/2}} A_3 (2\pi v_1) \left( \tilde{\beta}_1 - c^2 \tilde{\beta}_2 \alpha_2^{-1} B'_1 B_2^{-1} \right) \\ & + \alpha_3 \alpha_2^{-1} u^{1/2} B_3 (2\pi v_2) \left[ \tilde{\beta}_1 + \tilde{\beta}_2 \alpha_2^{-1} (a + b_1 + A_1) A_2^{-1} \right]. \end{aligned} \tag{88}$$

Equations 86–88 may now be used to obtain expressions for the three unknowns:  $\omega'_p$ ,  $\Omega'_p$ , and  $\lambda_s$ . From the definitions in Eqs. 52–53, it is seen that subtracting Eq. 87 from Eq. 86 gives  $\omega'_{p_i}$  as

$$\begin{aligned} \omega'_{p_i} = & 2\pi v_1 \left( t_i + \tilde{\beta}_1 - c^2 \tilde{\beta}_2 \alpha_2^{-1} B'_1 B_2^{-1} \right) \\ & - 2\pi v_2 \left[ t_i + \tilde{\beta}_1 + \tilde{\beta}_2 \alpha_2^{-1} (a + b_1 + A_1) A_2^{-1} \right]. \end{aligned} \tag{89}$$

Equation 88 already gives the negative of  $\Omega'_p$  so that  $\Omega'_{p_i}$  is determined as

$$\begin{aligned} \Omega'_{p_i} = & - \left( \tilde{\beta}_3 + \dot{h} t_i \right) \\ & + c^2 \frac{\alpha_3}{(-2\alpha_1)^{1/2}} A_3 (2\pi v_1) \left( \tilde{\beta}_1 - c^2 \tilde{\beta}_2 \alpha_2^{-1} B'_1 B_2^{-1} \right) \\ & - \alpha_3 \alpha_2^{-1} u^{1/2} B_3 (2\pi v_2) \left[ \tilde{\beta}_1 + \tilde{\beta}_2 \alpha_2^{-1} (a + b_1 + A_1) A_2^{-1} \right]. \end{aligned} \tag{90}$$

Lastly, adding Eq. 87 to  $K$  times Eq. 88 gives  $\lambda_{s_i}$  as

$$\begin{aligned} \lambda_{s_i} = & K \tilde{\beta}_3 + (2\pi v_2 + K \dot{h}) t_i \\ & - K c^2 \frac{\alpha_3}{(-2\alpha_1)^{1/2}} A_3 (2\pi v_1) \left( \tilde{\beta}_1 - c^2 \tilde{\beta}_2 \alpha_2^{-1} B'_1 B_2^{-1} \right) \\ & + \left( 1 + K \alpha_3 \alpha_2^{-1} u^{1/2} B_3 \right) (2\pi v_2) \left[ \tilde{\beta}_1 + \tilde{\beta}_2 \alpha_2^{-1} (a + b_1 + A_1) A_2^{-1} \right]. \end{aligned} \tag{91}$$

Equations 89 and 90 enable the computation of  $q_{1_s}$ ,  $q_{2_s}$ ,  $p_{1_s}$ , and  $p_{2_s}$  at time  $t_i$  through Eqs. 59 and 60, while  $\lambda_{s_i}$  is directly determined by Eq. 91. The spheroidal semilatus rectum,  $p$ , is already known because it is a constant of the motion in both classical and equinoctial elements; it is obtained from factoring the  $F(\rho)$  quartic.

## Propagating the Secular Parts of the Spheroidal Equinoctial Elements

It is now assumed that the secular oblate spheroidal equinoctial element set, which is defined as  $\mathbf{ae}_s = \{p, q_{1_s}, q_{2_s}, p_{1_s}, p_{2_s}, L_s\}$ , has been obtained somehow, either as given quantities or as a result of a transformation from ECI coordinates as described in the preceding sections. These secular elements are either constant or evolve with time according to the following formulas:

$$p(t) = p \quad (92)$$

$$\begin{bmatrix} q_{1_s}(t) \\ q_{2_s}(t) \end{bmatrix} = \begin{bmatrix} \cos[(\dot{g} + K\dot{h})\Delta t] & -\sin[(\dot{g} + K\dot{h})\Delta t] \\ \sin[(\dot{g} + K\dot{h})\Delta t] & \cos[(\dot{g} + K\dot{h})\Delta t] \end{bmatrix} \begin{bmatrix} q_{1_s}(t_i) \\ q_{2_s}(t_i) \end{bmatrix} \quad (93)$$

$$\begin{bmatrix} p_{1_s}(t) \\ p_{2_s}(t) \end{bmatrix} = \begin{bmatrix} \cos(\dot{h}\Delta t) & -\sin(\dot{h}\Delta t) \\ \sin(\dot{h}\Delta t) & \cos(\dot{h}\Delta t) \end{bmatrix} \begin{bmatrix} p_{1_s}(t_i) \\ p_{2_s}(t_i) \end{bmatrix} \quad (94)$$

$$\lambda_s(t) = \lambda_s(t_i) + (\dot{l} + \dot{g} + K\dot{h})\Delta t, \quad (95)$$

where

$$\Delta t = t - t_i. \quad (96)$$

Equation 95 shows  $\lambda_s$  evolving linearly with time.

## Solving the Generalized Kepler's Equation

The selected approach to solving the generalized Kepler's equation follows that of other authors, such as Getchell [17], where periodic terms are neglected in the first iteration. The complication is that the use of equinoctial elements means that all three kinematic equations are coupled.

For iteration  $j = 0$ , set  $\lambda_j = \lambda_s$ ,  $q_{1_j} = q_{1_s}$ ,  $q_{2_j} = q_{2_s}$ ,  $p_{1_j} = p_{1_s}$ , and  $p_{2_j} = p_{2_s}$ , and choose  $F_j = \lambda_j$  as an initial guess. Then, using a desired root-solving routine, solve the equinoctial form of Kepler's equation for Vinti theory:

$$\lambda_j = F_j - \gamma_1 q_{1_j} \sin F_j + \gamma_1 q_{2_j} \cos F_j, \quad (97)$$

where

$$\gamma_1 = \frac{a}{a_0} = \frac{a}{a + b_1} \leq 1. \quad (98)$$

The authors recommend a variable order Laguerre’s method [13]. Note in Eq. 98 that  $\gamma_1$  is Getchell’s notation [17]. Once converged on a value for  $F_j$ , obtain  $L_j$  by first computing the sine and cosine as

$$\sin L_j = \frac{(1 - q_{1j}^2 b_j) \sin F_j + q_{1j} q_{2j} b_j \cos F_j - q_{2j}}{1 - q_{1j} \cos F_j - q_{2j} \sin F_j} \tag{99}$$

$$\cos L_j = \frac{(1 - q_{2j}^2 b_j) \cos F_j + q_{1j} q_{2j} b_j \sin F_j - q_{1j}}{1 - q_{1j} \cos F_j - q_{2j} \sin F_j}, \tag{100}$$

where

$$b_j = \frac{1}{1 + \sqrt{1 - q_{1j}^2 - q_{2j}^2}}, \tag{101}$$

and then use the arctangent to compute  $L_j$  as

$$L_j = \text{atan2}(\sin L_j, \cos L_j). \tag{102}$$

Next, it is necessary to perform an update step to incorporate the periodic terms that were neglected earlier. These periodic components are  $\omega'_{pj}$ ,  $\Omega'_{pj}$ , and  $\lambda_{pj}$ , and they are calculable from the available quantities, which consist of some variables but mostly constants. First, compute  $l_j + \omega'_j + K\Omega'_j$  as

$$\begin{aligned} l_j + \omega'_j + K\Omega'_j = & 2\pi v_1 \\ & \times \left\{ \frac{1}{(-2\alpha_1)^{1/2}} \left[ b_1 F_j + a (F_j - q_{1j} \sin F_j + q_{2j} \cos F_j) \right. \right. \\ & \left. \left. + A_1 L_j + \sum_{k=1}^2 \tilde{A}_{1k} \tilde{q}_k (q_{1j}, q_{2j}, L_j) \right] \right. \\ & \left. + c^2 \frac{u^{1/2}}{\alpha_2} \left[ B'_1 L_j + \sum_{k=1}^2 \tilde{B}_{1(2k)} \tilde{p}(2k) (p_{1j}, p_{2j}, L_j) \right] \right. \\ & \left. + c^2 \frac{B'_1}{B_2 (-2\alpha_1)^{1/2}} \left[ A_2 L_j + \sum_{k=1}^4 \tilde{A}_{2k} \tilde{q}_k (q_{1j}, q_{2j}, L_j) \right] \right. \\ & \left. - c^2 \frac{B'_1 u^{1/2}}{B_2 \alpha_2} \left[ B_2 L_j + \sum_{k=1}^2 \tilde{B}_{2(2k)} \tilde{p}(2k) (p_{1j}, p_{2j}, L_j) \right] \right\}, \tag{103} \end{aligned}$$

which is analogous to Eq. 86, and then compute  $l_j + g_j + K\Omega'_j$  as

$$\begin{aligned}
 l_j + g_j + K\Omega'_j &= 2\pi v_2 \\
 &\times \left\{ \frac{1}{(-2\alpha_1)^{1/2}} \left[ b_1 F_j + a (F_j - q_{1j} \sin F_j + q_{2j} \cos F_j) \right. \right. \\
 &\quad \left. \left. + A_1 L_j + \sum_{k=1}^2 \tilde{A}_{1k} \tilde{q}_k (q_{1j}, q_{2j}, L_j) \right] \right. \\
 &\quad \left. + c^2 \frac{u^{1/2}}{\alpha_2} \left[ B'_1 L_j + \sum_{k=1}^2 \tilde{B}_{1(2k)} \tilde{p}(2k) (p_{1j}, p_{2j}, L_j) \right] \right. \\
 &\quad \left. - \frac{a + b_1 + A_1}{A_2 (-2\alpha_1)^{1/2}} \left[ A_2 L_j + \sum_{k=1}^4 \tilde{A}_{2k} \tilde{q}_k (q_{1j}, q_{2j}, L_j) \right] \right. \\
 &\quad \left. + \frac{(a + b_1 + A_1) u^{1/2}}{A_2 \alpha_2} \right. \\
 &\quad \left. \times \left[ B_2 L_j + \sum_{k=1}^2 \tilde{B}_{2(2k)} \tilde{p}(2k) (p_{1j}, p_{2j}, L_j) \right] \right\}, \quad (104)
 \end{aligned}$$

which is analogous to Eq. 87. It follows that  $\omega'_{p_j}$  can be determined as

$$\omega'_{p_j} = (l_j + \omega'_j + K\Omega'_j) - (l_j + g_j + K\Omega'_j), \quad (105)$$

$\Omega'_{p_j}$  as

$$\begin{aligned}
 \Omega'_{p_j} &= -c^2 \alpha_3 (-2\alpha_1)^{-1/2} \left[ A_3 L_j + \sum_{k=1}^4 \tilde{A}_{3k} \tilde{q}_k (q_{1j}, q_{2j}, L_j) \right] \\
 &\quad + \alpha_3 \alpha_2^{-1} u^{1/2} \left[ B_3 L_j + \tilde{B}_{32} \tilde{p}_2 (p_{1j}, p_{2j}, L_j) \right] \\
 &\quad + c^2 \alpha_3 (-2\alpha_1)^{-1/2} A_3 (l_j + \omega'_j + K\Omega'_j) \\
 &\quad - \alpha_3 \alpha_2^{-1} u^{1/2} B_3 (l_j + g_j + K\Omega'_j), \quad (106)
 \end{aligned}$$

and  $\lambda_{p_j}$  as

$$\begin{aligned}
 \lambda_{p_j} &= \frac{a + b_1 + A_1}{a + b_1} (\omega'_{p_j} + K\Omega'_{p_j}) + c^2 \frac{(-2\alpha_1)^{1/2} u^{1/2}}{\alpha_2 (a + b_1)} B'_1 K \Omega'_{p_j} \\
 &\quad - \frac{1}{a + b_1} \left[ A_1 (L_j - \lambda_s) + \sum_{k=1}^2 \tilde{A}_{1k} \tilde{q}_k (q_{1j}, q_{2j}, L_j) \right] \\
 &\quad - c^2 \frac{(-2\alpha_1)^{1/2} u^{1/2}}{\alpha_2 (a + b_1)} \left[ B'_1 (L_j - \lambda_s) + \sum_{k=1}^2 \tilde{B}_{1(2k)} \tilde{p}(2k) (p_{1j}, p_{2j}, L_j) \right]. \quad (107)
 \end{aligned}$$

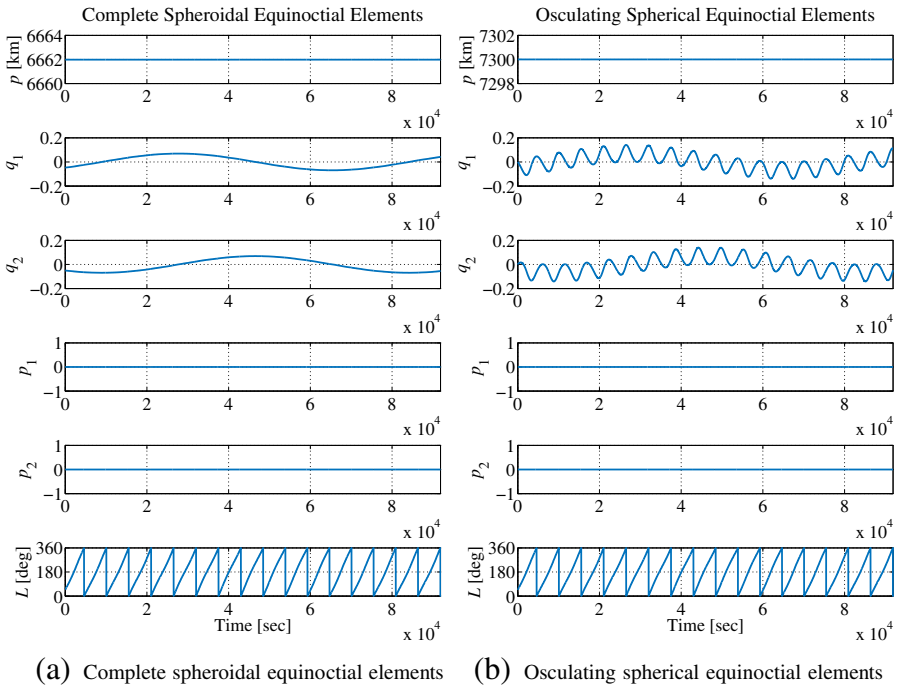


**Fig. 3** Example 1: Side-by-side comparison of spheroidal and spherical equinoctial elements for a nominally circular equatorial Vinti trajectory evolving over roughly 18 orbits with  $J_2 = 5.08 \times 10^{-2}$

Then  $q_{1j}$  and  $q_{2j}$  can be updated with the inverse of Eq. 59 and  $p_{1j}$  and  $p_{2j}$  can be updated with the inverse of Eq. 60. The whole process is then repeated until converged by returning to Eq. 97, setting  $j = j + 1$ ,  $\lambda_j = \lambda_s + \lambda_{p_j}$ , and choosing  $F_j = \lambda_j$  as an initial guess. The algorithm concludes when convergence is achieved to a desired tolerance. A companion code for the OS equinoctial Vinti propagator is provided as an Online Resource.<sup>3</sup>

### Examples

Two examples are explored in this section, one at Earth and one at Saturn. The accuracy of Vinti dynamics relative to low-fidelity spherical harmonic representations was assessed in prior work [1, 5] and is not discussed here. Instead, the opportunity is taken to focus on the capabilities of the analytical propagator and the geometric interpretation of the new element set.

Example 1 investigates how the equinoctial elements evolve over approximately 18 orbits for a nominally circular equatorial low Earth orbit (LEO) case with an initial periapsis radius of  $r_p = 7,300$  km. To better spotlight the disparity between

<sup>3</sup>Code updates will be available from this website: <http://sites.utexas.edu/russell/publications/code/vinti/>

the spheroidal and spherical elements, oblateness is exaggerated an order of magnitude above Earth's by setting  $J_2 = 5.08 \times 10^{-2}$ . Figure 3a shows the spheroidal elements and Fig. 3b the spherical elements. These plots are overlaid in Fig. 4 to emphasize the short-periodic averaging effect. The spherical elements are obtained by numerically integrating Hamilton's equations of motion under the Vinti potential and transforming from ECI coordinates to osculating spherical elements.

With this comparison, it is possible to interpret a geometric relationship between spheroidal and spherical elements. The last three elements appear almost indistinguishable from each other, but the first three are remarkably different. While the spherical  $p$  is constant and maintains the value of 7,300 km, the spheroidal  $p$ , which is strictly a constant of the motion, is notably almost 640 km smaller. The spherical  $p$  is constant because the orbit is equatorial. The long-periodic effects evident in the spheroidal  $q_1$  and  $q_2$  agree with those of their spherical counterparts. Note that the long-periodic effect in  $q_1$  and  $q_2$  is an artifact of representing the eccentricity vector in vector components, not from the traditional notion found in perturbation theory. In fact, long-periodic terms do not exist under the Vinti potential [27] and may be considered absorbed into the coordinates; the short-periodic effects are orders of magnitude smaller than for the spherical elements. In the spherical  $q$ 's, the short-periodic effects are a consequence of the short-periodic variations in spherical eccentricity. These short-periodic effects do not appear in the spheroidal  $q$ 's because, like the spheroidal semilatus rectum, the spheroidal eccentricity is a constant of the motion. The spheroidal  $q$ 's appear to track the short-periodic average of the spherical  $q$ 's, but this is an artifact of the spheroidal coordinate transformation. Solving

**Fig. 4** Example 1: Complete spheroidal equinoctial elements overlaid on the osculating spherical elements

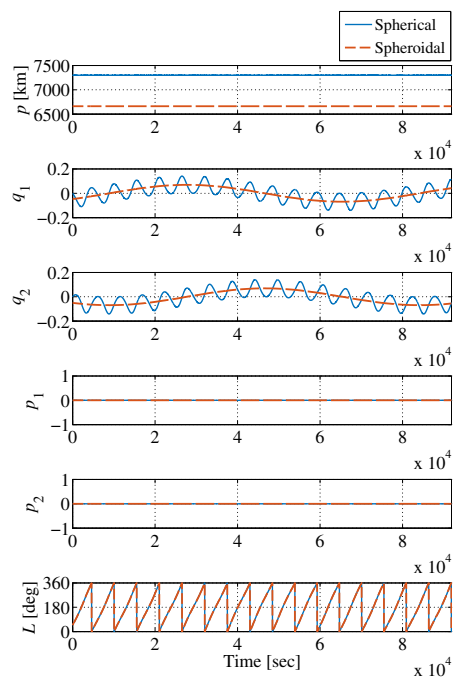
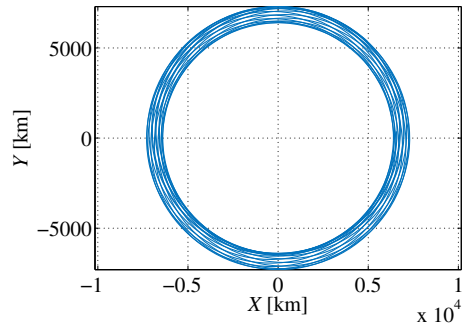


**Fig. 5** Example 1: Vinti trajectory in the ECI frame for a nominally circular equatorial orbit with  $J_2 = 5.08 \times 10^{-2}$ , looking down on the equatorial plane



the Vinti problem does not invoke any averaging techniques, as the spheroidal  $p$  is clearly not an average of the spherical  $p$ . The effective averaging of short-periodic variations generally applies to  $p_1$ ,  $p_2$ , and  $L$  as well, but the effects are not visible for the particular example in Fig. 3. Even if the orbit were inclined in this example, the amplitude of the short-periodic variations would be on a much smaller scale than the amplitude of the long-periodic variations for these three elements; the averaging effect would still not be apparent in a comparison similar to Fig. 3. Figure 5 illustrates the associated Vinti trajectory in the ECI frame.

Example 2 moves the focus toward Saturn, where certain phases of mission design based on two-body dynamics are known to fail due to Saturn’s highly oblate

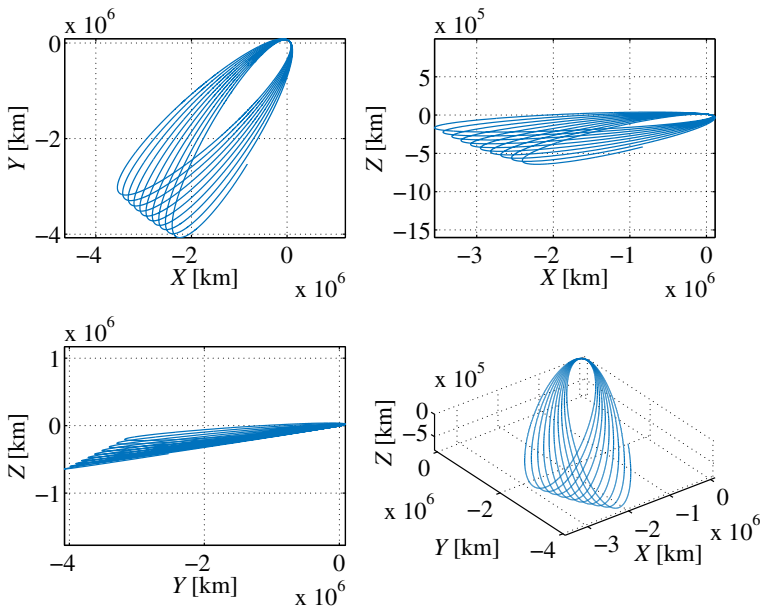
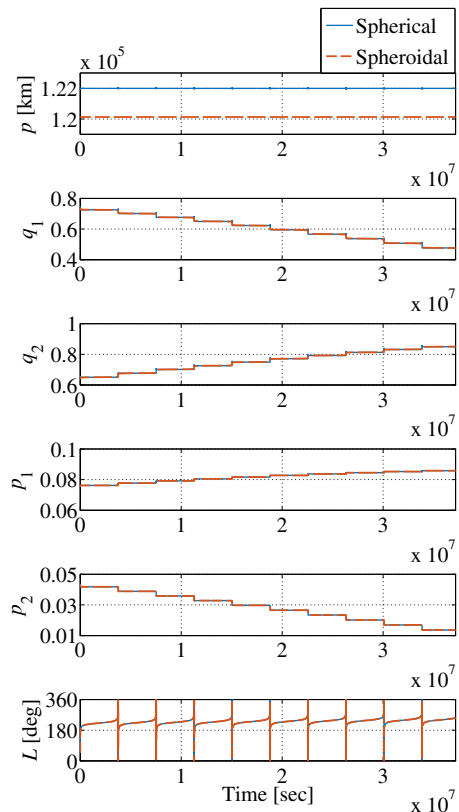


**Fig. 6** Example 2: Vinti trajectory in the Saturn-centered inertial frame for a Saturn orbit insertion scenario. The first three panes show the trajectory projected onto three different orthogonal planes and the bottom-right pane shows the 3D trajectory

shape [9]. The current example investigates Saturn orbit insertion using the Vinti potential. Figure 6 illustrates the associated Vinti trajectory in the Saturn-centered inertial frame. The trajectory is shown in the bottom-right pane. To clarify the perspective, the first three panes show the trajectory projected onto three different orthogonal planes. Gravity field data is taken from Jacobson et al. [20], where  $J_2 \approx 1.6291 \times 10^{-2}$  and  $J_4 \approx 9.36 \times 10^{-4}$ . Recall that the Vinti potential captures approximately 72% of  $J_4$  for the Earth. At Saturn, the Vinti potential captures roughly 28% of  $J_4$ . Other parameter values used are  $\mu = 3.7931 \times 10^7 \text{ km}^3/\text{s}^2$  and  $R_e = 60,330 \text{ km}$ . Initial osculating spherical orbit parameters are chosen as  $r_p = 61,330 \text{ km}$ ,  $e_K = 0.99$ ,  $I_K = 10^\circ$ ,  $\Omega_K = 30^\circ$ ,  $\omega_K = 11^\circ$ ,  $f_K = 6^\circ$ . The subscript “K” denotes Keplerian as opposed to spheroidal orbital elements. The simulation is carried out for a little over a year (about 10 revolutions) to visualize the long-term effects on the orbit. A comparison of spheroidal and spherical elements is shown in Fig. 7. While the short-periodic averaging effects still exist, at this scale, they are not apparent and the last five spheroidal and spherical elements have similar values. Again, the semilatus rectum is seen to be distinctly different between the spheroidal and spherical elements. Since the eccentricity is quite high, the eccentricity and node vector components experience what looks like a step function at each

**Fig. 7** Example 2: Comparison of spheroidal and spherical equinoctial elements for a Saturn orbit insertion scenario, propagated over roughly 10 revolutions





periapsis passage, when the effects of oblateness are much stronger. For the same reason, the true longitude is very nonlinear in time. The angle moves rapidly through periapsis, resulting in the observed heartbeat characteristic. Note that after one year, the effect of neglecting 72% of  $J_4$  will manifest itself as a sizable phase error. For the much shorter duration of orbit insertion, however, the phase error will not accumulate significantly and the Vinti trajectory offers a good approximation.

Given the complexity of a Vinti propagator, any means of validating an implementation is valuable to practitioners. The constants of the motion can fulfill this role in principle. However, the authors found that their properties are not adequately preserved if traditional approximations are used, assuming inputs and outputs are desired in inertial position and velocity. The constants are preserved to double precision or about 15 digits only when the exact expression for  $\dot{\Omega}'$  is used, which was developed recently by the authors [4]. When performing transformations near a pole, the approximation proposed in that study still preserves the constants of the motion. The symmetry of the Vinti problem also causes the total angular momentum to be conserved for an equatorial orbit, an important corner case.

## Conclusions

A nonsingular analytical solution to the unperturbed Vinti problem is presented for bounded orbits. The method avoids the angle ambiguities of classical orbital elements by solving the problem in oblate spheroidal equinoctial orbital elements, the generalization of traditional equinoctial elements to an oblate spheroidal geometry. New geometric interpretations of spheroidal elements are also discussed. Innate to the geometrical description in these coordinates, five of the oblate spheroidal equinoctial elements appear to naturally track the singly averaged value of the spherical equinoctial elements. The constant element is the spheroidal semilatus rectum, which in general is not the average of its spherical counterpart. While the examples considered scenarios with large  $J_2$  values to illustrate geometric features, oblateness is generally important for real missions, as for the Earth and most other bodies. Such an analytical solution may be useful in preliminary mission design as a more accurate starting point relative to a two-body-based solution, offering increased accuracy for bounded orbits, including in the vicinity of the critical inclination. This solution also enables future work on the study of perturbations through the variational equations, and, being nonsingular for bounded orbits, prescribes an analytical state transition matrix (STM) that is nonsingular in regimes where some of the previous analytical STMs based on Vinti theory have been singular.

**Acknowledgements** The authors thank Paul Schumacher for the encouragement to continue pursuing the development of the equinoctial elements for Vinti theory. The authors are also grateful to AFRL for support that initiated this work.

## Compliance with Ethical Standards

**Conflict of Interest** On behalf of all authors, the corresponding author states that there is no conflict of interest.

## References

1. Biria, A.D.: Revisiting Vinti theory: generalized equinoctial elements and applications to spacecraft relative motion. PhD thesis, Supervisor: Dr. Ryan P. Russell. The University of Texas at Austin, Austin (2017)
2. Biria, A.D., Russell, R.P.: A satellite relative motion model including  $J_2$  and  $J_3$  via Vinti's intermediary. In: AAS/AIAA Space Flight Mechanics Meeting, Univelt, Inc., San Diego, CA, Advances in the Astronautical Sciences, vol 158, pp 3475–3494, Paper AAS 16-537 (2016)
3. Biria, A.D., Russell, R.P.: Equinoctial elements for Vinti theory: generalizations to an oblate spheroidal geometry. In: International Workshop on Satellite Constellations and Formation Flying, Boulder, Paper IWSCFF 17-75 (2017)
4. Biria, A.D., Russell, R.P.: Equinoctial elements for Vinti theory: generalizations to an oblate spheroidal geometry. *Acta Astronaut.* **153**, 274–288 (2018). <https://doi.org/10.1016/j.actaastro.2017.11.013>
5. Biria, A.D., Russell, R.P.: A satellite relative motion model including  $J_2$  and  $J_3$  via Vinti's intermediary. *Celest. Mech. Dyn. Astron.* **130**(3) (2018b). <https://doi.org/10.1007/s10569-017-9806-4>
6. Biscani, F., Izzo, D.: A complete and explicit solution to the three-dimensional problem of two fixed centres. *Mon. Not. R. Astron. Soc.* **455**(4), 3480–3493 (2016). <https://doi.org/10.1093/mnras/stv2512>
7. Broucke, R.A., Cefola, P.J.: On the equinoctial orbit elements. *Celest. Mech.* **5**(3), 303–310 (1972). <https://doi.org/10.1007/BF01228432>
8. Brouwer, D., Clemence, G.M.: *Methods of Celestial Mechanics*. Academic Press, New York (1961)
9. Buffington, B., Strange, N.J.: Patched-integrated gravity-assist trajectory design. In: AAS/AIAA Astrodynamics Specialist Conference, Paper AAS 07-276, vol. 129, pp. 2053–2072. Univelt, Inc., San Diego (2008)
10. Conway, B.A.: An improved algorithm due to Laguerre for the solution of Kepler's equation. *Celest. Mech.* **39**(2), 199–211 (1986). <https://doi.org/10.1007/BF01230852>
11. Danielson, D.A., Sagovac, C.P., Neta, B., Early, L.W.: *Seminanalytic satellite theory*. Tech. Rep. NPS Report NPS-MA-95-002, Naval Postgraduate School Department of Mathematics, Monterey (1995)
12. Deprit, A., Ferrer, S.: Note on Cid's radial intermediary and the method of averaging. *Celest. Mech.* **40**(3), 335–343 (1987). <https://doi.org/10.1007/BF01235851>
13. Der, G.J.: The superior Lambert algorithm. In: *Advanced Maui Optical and Space Surveillance Technologies (AMOS) Conference*. Maui (2011)
14. Der, G.J., Bonavito, N.L. (eds.): *Orbital and Celestial Mechanics, Progress in Astronautics and Aeronautics, vol. 177*. American Institute of Aeronautics and Astronautics, Reston (1998)
15. Fernández, J.M., Floría, L.: New intermediaries for the main problem in satellite theory. *Int. Astron. Union Colloq.* **132**, 341–352 (1993). <https://doi.org/10.1017/S0252921100066239>
16. Garfinkel, B., Aksnes, K.: Spherical coordinate intermediaries for an artificial satellite. *Astron. J.* **75**(1), 85–91 (1970). <https://doi.org/10.1086/110946>
17. Getchell, B.C.: Orbit computation with the Vinti potential and universal variables. *J. Spacecr. Rocket.* **7**(4), 405–408 (1970). <https://doi.org/10.2514/3.29954>
18. Gim, D.W., Alfriend, K.T.: Satellite relative motion using differential equinoctial elements. *Celest. Mech. Dyn. Astron.* **92**(4), 295–336 (2005). <https://doi.org/10.1007/s10569-004-1799-0>
19. Izsak, I.G.: On the critical inclination in satellite theory. Tech. rep. Smithsonian Institution Astrophysical Observatory, special Report No. 90 (1962)
20. Jacobson, R.A., Antreasian, P.G., Bordi, J.J., Criddle, K.E., Ionasescu, R., Jones, J.B., Mackenzie, R.A., Meek, M.C., Parcher, D., Pelletier, F.J., Owen, W.M. Jr., Roth, D.C., Roundhill, I.M., Stauch, J.R.: The gravity field of the saturnian system from satellite observations and spacecraft tracking data. *Astron. J.* **132**(6), 2520–2526 (2006). <https://doi.org/10.1086/508812>
21. Lara, M., Gurfil, P.: Integrable approximation of  $J_2$ -perturbed relative orbits. *Celest. Mech. Dyn. Astron.* **114**(3), 229–254 (2012). <https://doi.org/10.1007/s10569-012-9437-8>
22. Nayfeh, A.H.: *Perturbation Methods*. Wiley-VCH Verlag GmbH & Co. KGaA, Weinheim (2004)
23. Vinti, J.P.: New method of solution for unretarded satellite orbits. *J. Res. Natl. Bur. Stand.* **63B**(2), 105–116 (1959). <https://doi.org/10.6028/jres.063B.012>
24. Vinti, J.P.: Theory of an accurate intermediary orbit for satellite astronomy. *J. Res. Natl. Bur. Stand.* **65B**(3), 169–201 (1961). <https://doi.org/10.6028/jres.065B.017>
25. Vinti, J.P.: Intermediary equatorial orbits of an artificial satellite. *J. Res. Natl. Bur. Stand.* **66B**(1), 5–13 (1962). <https://doi.org/10.6028/jres.066B.002>

26. Vinti, J.P.: Zonal harmonic perturbations of an accurate reference orbit of an artificial satellite. *J. Res. Natl. Bur. Stand.* **67B**(4), 191–222 (1963). <https://doi.org/10.6028/jres.067B.016>
27. Vinti, J.P.: Inclusion of the third zonal harmonic in an accurate reference orbit of an artificial satellite. *J. Res. Natl. Bur. Stand.* **70B**(1), 17–46 (1966). <https://doi.org/10.6028/jres.070B.003>
28. Vinti, J.P.: Invariant properties of the spheroidal potential of an oblate planet. *J. Res. Natl. Bur. Stand.* **70B**(1), 1–16 (1966). <https://doi.org/10.6028/jres.070B.002>
29. Vinti, J.P.: Improvement of the spheroidal method for artificial satellites. *Astron. J.* **74**(1), 25–34 (1969). <https://doi.org/10.1086/110770>
30. Walden, H., Watson, S.: Differential corrections applied to Vinti's accurate reference satellite orbit with inclusion of the third zonal harmonic. Tech. Rep. TN D-4088. National Aeronautics and Space Administration, Washington DC (1967)
31. Walker, M.J.H., Ireland, B., Owens, J.: A set of modified equinoctial orbit elements. *Celest. Mech.* **36**(4), 409–419 (1985). <https://doi.org/10.1007/BF01227493>
32. Wiesel, W.E.: Numerical solution to Vinti's problem. *J. Guid. Control. Dyn.* **38**(9), 1757–1764 (2015). <https://doi.org/10.2514/1.G000661>
33. Wright, S.P.: Orbit determination using Vinti's solution. PhD thesis, Supervisor: Dr. William E. Wiesel, Air Force Institute of Technology, Wright-Patterson Air Force Base (2016)
34. Wu, L., Tong, F.: A third-order solution of Vinti's problem with explicit expressions for the Poisson brackets. *Chin. Astron. Astrophys.* **5**(2), 192–201 (1981). [https://doi.org/10.1016/0275-1062\(81\)90031-X](https://doi.org/10.1016/0275-1062(81)90031-X)
35. Zurita, L.D.: Orbital resonances in the Vinti solution. In: Advanced Maui Optical and Space Surveillance Technologies (AMOS) Conference, Maui (2017)

**Publisher's Note** Springer Nature remains neutral with regard to jurisdictional claims in published maps and institutional affiliations.